Title: Lateral adhesion drives reintegration of misplaced cells into epithelial monolayers

Authors: Dan T. Bergstralh*, Holly E. Lovegrove*, Daniel St Johnston

Affiliations: The Gurdon Institute and the Department of Genetics, University of Cambridge, Tennis Court Road, Cambridge CB2 1QN, UK
Correspondence should be addressed to DStJ.
* These authors contributed equally to this work.

Cells in simple epithelia orient their mitotic spindles in the plane of the epithelium so that both daughter cells are born within the epithelial sheet. This is assumed to be important to maintain epithelial integrity and prevent hyperplasia, because misaligned divisions give rise to cells outside the epithelium[1,2]. Here we test this assumption in three types of *Drosophila* epithelia; the cuboidal follicle epithelium, the columnar early embryonic ectoderm, and the pseudostratified neuroepithelium. Ectopic expression of Inscuteable in these tissues reorients mitotic spindles, resulting in one daughter cell being born outside of the epithelial layer. Live imaging reveals that these misplaced cells reintegrate into the tissue. Reducing the levels of the lateral homophilic adhesion molecules Neuroglian or Fasciclin 2 disrupts reintegration, giving rise to extra-epithelial cells, whereas disruption of adherens junctions has no effect. Thus, the reinsertion of misplaced cells appears to be driven by lateral adhesion, which pulls cells born outside the epithelia layer back into it. Our findings reveal a robust mechanism that protects epithelia against the consequences of misoriented divisions.

Previous work demonstrated that metaphase spindles in the cuboidal follicle epithelium are oriented between 0° and 35° relative to the plane of the layer, roughly perpendicular to the apical-basal axis of the cell[3]. Metaphase spindle orientation in this tissue relies on the canonical factors Mud and Pins, and mutants in either gene randomize spindle orientation[4]. Unexpectedly, we found that the organisation of the epithelium is maintained in *mud* and *pins* mutants (Fig. 1A and Supplementary Fig. 1A). This is not

due to post-metaphase correction of division angles, as vertically-oriented spindles persist into telophase in *mud* mutants (Fig. 1B).

To disrupt spindle orientation more severely, we ectopically expressed Inscuteable in follicle cells. In neuroblasts, this protein recruits Pins and Mud to the apical cortex of neuroblasts so that mitotic spindles are oriented along the apical-basal axis[5-9]. It has a similar effect on spindle orientation when ectopically expressed in follicle cells (Fig. 1C). Rather than randomizing spindle orientation as in *pins* and *mud* mutants, Inscuteable orients almost all spindles perpendicular to the epithelial plane (Fig. 1D). Divisions are thus horizontal and produce an apical and a basal daughter (Supplementary Fig. 1B). Like spindle randomization, this has no effect on tissue organisation (Figs. 1C, 1E and Supplementary Fig. 1C). In the neuroblast, spindle orientation controls cell fate by ensuring the asymmetric segregation of fate determinants to one daughter cell. Inscuteable expression in the follicle epithelium does not confer neural cell fate, since it does not cause expression of the transcription factor Deadpan (Supplementary Fig. 1D). We also observed that female flies expressing UAS-Inscuteable under the control of the strong follicle cell driver Traffic Jam-Gal4 are fertile (not shown), indicating that reorienting most divisions in the follicular epithelium does not disrupt egg chamber development.

In the imaginal wing disc, misoriented cell division is associated with basal cell extrusion and apoptosis[10,11]. We therefore considered the possibility that the apically misplaced cells produced by horizontal divisions in the follicle cell layer are also eliminated by programmed cell death. However, misplaced cells show neither cleaved caspase-3 immunoreactivity nor pyknosis (Supplementary Fig. 1E). Furthermore, expression of the apoptotic inhibitor p35 has no effect on follicular epithelia expressing Inscuteable (n=17 ovarioles from 6 dissected flies) or containing $pins^{p62}$ mutant clones (n=12 clones larger than 5 cells) (Supplementary Fig. 1F,G). Live imaging reveals that rather than dying, misplaced daughter cells simply reintegrate back into the epithelial monolayer (Fig. 1F and Supplementary Movie 1).

Our findings prompted a closer examination of mitosis in wild type follicle cells. These cells only divide during the early stages of egg chamber maturation, switching from mitosis to endocycling at stage 6. Live imaging reveals that the monolayer has an

uneven, "bubbly" appearance in early stages (Supplementary Fig. 2A). This is because mitotic cells round up, exhibiting a concomitant increase in cortical phospho-myosin (Supplementary Figure 2B), and often move apically, pulling away from the basement membrane (Fig. 2A,B). Daughter cells are frequently born detached from the basement membrane (Fig. 2C and Supplementary Figure 2C). These cells then reinsert into the monolayer (Fig. 2D and Supplementary Movie 2). These results are consistent with the earlier observation that metaphase spindle angles, which determine the angle of division, are not strictly parallel to the plane of the tissue. They also show that in the follicle epithelium reintegration is not only a backup mechanism, but occurs as a normal feature of division. We speculate that apical movement and angled cell divisions may help to relieve local tension caused by cell expansion and division, which crowds the tightly-packed neighboring cells.

Reintegration of newly-born epithelial cells has previously been observed in two specific developmental contexts. In mammalian uteric buds, cells move apically into the lumen to divide and one daughter cell then re-inserts into the epithelium at a distant site[12]. This may contribute to branching. Secondly, neuroepithelial cells of the zebrafish neural keel normally orient their spindles vertically, and the apical daughter then intercalates into the opposite side of the neural tube in a process that depends on planar cell polarity signaling[13]. In both of these cases, reintegration occurs at a distant site. In contrast, reintegration in the follicle epithelium is always local, and therefore acts to maintain, rather than to alter, epithelial architecture.

Since local reintegration can only be detected by live imaging, it is possible that it is a general feature of epithelial tissues that has been largely overlooked. To test this possibility, we examined two other types of *Drosophila* epithelia: the columnar epithelium of the early embryonic ectoderm and the neuroepithelium of the developing optic lobe. It has previously been shown that ectopic expression of Inscuteable reorients spindles in these tissues without affecting tissue integrity (Fig. 3A,B)[5,6,14]. The neuroepithelium is pseudostratified and undergoes interkinetic nuclear migration prior to division[14,15]. Expression of Inscuteable in this tissue efficiently reorients divisions, producing one daughter cell that protrudes apically from the layer, as in the follicular epithelium (Fig. 3C). Live imaging reveals that these apical cells then reintegrate into the

epithelium over the next 30 minutes (Fig. 3C, Supplementary Fig. 3A, and Supplementary Movie 3). Inscuteable expression also causes misoriented divisions in the columnar cells of the early embryonic ectoderm, resulting in misplaced daughter cells that lie below, rather than above, the monolayer (Supplementary Fig. 3B,C). 3D tracking over time shows that these basally-misplaced daughter cells can move apically to reintegrate (Fig. 3D and Supplementary Fig. 3D).

Reintegration appears to be an active process, since cells undergo a series of shape changes as they reinsert into the monolayer (Fig. 4A and Supplemental Movie 4). One possibility is that this is a cell migration process driven by actomyosin constriction at the rear (the apical surface), which squeezes the basal side of the cell back into the epithelium. However, we did not observe an obvious enrichment of the Myosin Regulatory Light Chain (Spaghetti Squash) or Heavy Chain (Zipper) at the apical surface of reintegrating cells (Fig. 4B, Supplementary Fig. 4A, and Supplemental Movie 5). Myosin is most obviously enriched at the adherens junctions. This correlates with a planar constriction of the reintegrating cell at this level, which would be predicted to hinder rather than help reintegration. Furthermore, reintegrating cells often show a large, transient expansion of their apical free surface, which suggests that the apical membrane is pushed out to accommodate the compression of the basal side of the cell as it squeezes between its neighbours (Supplementary Fig. 4B). This behavior is incompatible with a reintegration mechanism initiated by a contractile force at the rear of the cell, although myosin may play a role in retracting the apical projection during the final stages of reintegration.

These observations raise the question of how cells born above or below the monolayer are induced to move in the correct direction to reintegrate. We observed previously that the apical polarity factors aPKC, Bazooka, and Crumbs disappear from the apical cortex of the follicle cells during mitosis, so it is unlikely that they act as polarity cues for reintegration[4]. Similarly, misplaced cells have no obvious attachment to the basement membrane, and there is no evidence that they form basal stalks, which in any case would be inherited only by the basal daughter of a horizontal division. In *Drosophila,* cadherin-based adherens junctions localize to the apical side of the lateral membrane, in contrast to mammals where they lie more basally. Cells born apical to the

epithelium remain attached to the monolayer by these apical adherens junctions, as revealed by Armadillo (*Drosophila* β-Catenin) staining (Fig. 4C). In wild type tissues, both daughter cells inherit part of the apical belt of adherens junctions from the mother cell, whereas the more apical daughter inherits all of the adherens junctions following a horizontal division[16,17] (Supplementary Fig. 4C). Live imaging reveals that the basal cell generates a new junction with its sister and a transient junction that extends along its lateral cortex (Fig. 4D and Supplementary Movie 6). Thus, adherens junctions link both apical and basal daughters to cells within the epithelium.

To test for a role for adherens junctions in reintegration, we used the strong hypomorphic allele *armadillo*^{3} (previously called *arm*^{XP33}) which encodes a truncated protein and causes intermittent gaps in the epithelium[18]. We were unable to detect misplaced cells or multilayering in *arm*^{3} clones expressing Inscuteable (n = 15 mutant clones of at least 6 cells) and observed no cell death (Fig. 4E). Reintegration of an *arm*^{3} mutant cell expressing Inscuteable was also observed directly (Supplementary Fig. 4D). These results argue against a major role for adherens junctions in this process.

In addition to their apicolateral adherens junctions, follicle cells adhere laterally through functionally-redundant homophilic adhesion molecules, such as the IgCAM Neuroglian[167] (Nrg[167]) and the N-Cam-like protein Fasciclin II (Fas2)[19,20]. Both Nrg[167] and Fas2 are highly expressed along the length of follicle cell lateral membranes during the first half of oogenesis, when follicle cells are dividing, but their expression is down-regulated in post-mitotic stages (Fig. 5A,B)[21]. This pattern of expression suggests that these proteins are important during division. They are also expressed along lateral membranes in the embryonic epithelium and neuroepithelium (Supplementary Fig. 5A,B). Furthermore, Nrg is localised along the cortex throughout the course of reintegration (Supplementary Movie 7).

In agreement with earlier work, shRNA-mediated depletion of Nrg[167] causes the appearance of occassional follicle cells lying apical to the epithelial monolayer, which is otherwise unperturbed (Fig. 5C)[22]. Apical cells are also observed in mutant clones of *Fas2*^{G0336}, a P-element allele that behaves as a protein null (Fig. 5D and Supplementary Fig. 5C)[23]. Similar phenotypes have been previously attributed to the loss of apical-basal polarity, but the Nrg shRNA and *Fas2* mutant cells within the monolayer appear to have

normal polarity, as shown by the wild-type distributions of aPKC, Par-6, Bazooka, DE-cadherin, Arm and Dlg (Supplementary Figure 5D-I)[24]. We therefore hypothesized that the apically extruded cells represent failed reintegrations. To test this possibility, we increased the number of cells born above the layer by overexpressing Inscuteable in *Nrg* knockdown or *Fas2* mutant cells. Inscuteable expression increased the mean number of apically-positioned cells more than twofold when combined with Nrg-shRNA and more than ten-fold in $Fas2^{G0336}$ mutant egg chambers (Fig. 5E,F, and H). Live imaging confirmed that cells born apically remain above the epithelium and never reintegrate (Fig. 5G, Supplementary Movie 8 and Supplementary Fig. 5J). Cumulatively, these results show that normal levels of lateral adhesion are required for reintegration.

Based on these results, we propose that tissue surface tension drives reintegration by acting to maximize cell-cell adhesion (Fig. 5I)[25]. Because this process is driven by lateral adhesion, it should be able to pull cells back into the monolayer from either side of the epithelium, and this may explain how misplaced cells in the embryonic ectoderm reintegrate from the basal side, whereas follicle and optic lobe cells reintegrate from the apical side. Although these three epithelia reintegrate misplaced cells, this does not appear to be the case in the wing disc epithelium[11]. This difference may arise because lateral adhesion molecules like Neuroglian are concentrated in apical septate junctions in the wing disc, rather than along the entire lateral membrane as seen in most other mitotic epithelia. These lateral adhesion proteins will therefore segregate into only the apical daughter of a horizontal division in the wing disc, thereby preventing the basal daughter from integrating by maximizing lateral adhesion[26].

Contrary to expectation, spindle misorientation does not disrupt the organisation of typical cuboidal, columnar or pseudostratified epithelia in *Drosophila*. Instead, misplaced cells reintegrate, providing a robust mechanism to protect epithelial monolayers from the consequences of misoriented divisions. Indeed, this mechanism may act more generally to safeguard epithelia against any processes that might disrupt their organisation. It will therefore be interesting to investigate whether reintegration also occurs in vertebrate epithelia, where the major lateral adhesion molecule is E-cadherin, and whether a role in reintegration contributes to E-cadherin's function as a tumour suppressor.

References:

1. Pease, J. C. & Tirnauer, J. S. Mitotic spindle misorientation in cancer--out of alignment and into the fire. *J Cell Sci* **124,** 1007–1016 (2011).
2. McCaffrey, L. M. & Macara, I. G. Epithelial organization, cell polarity and tumorigenesis. *Trends Cell Biol* **21,** 727–735 (2011).
3. Fernández-Miñán, A., Martín-Bermudo, M. D. & González-Reyes, A. Integrin signaling regulates spindle orientation in Drosophila to preserve the follicular-epithelium monolayer. *Curr Biol* **17,** 683–688 (2007).
4. Bergstralh, D. T., Lovegrove, H. E. & St Johnston, D. Discs large links spindle orientation to apical-Basal polarity in Drosophila epithelia. *Curr Biol* **23,** 1707–1712 (2013).
5. Kraut, R., Chia, W., Jan, L. Y., Jan, Y. N. & Knoblich, J. A. Role of inscuteable in orienting asymmetric cell divisions in Drosophila. *Nature* **383,** 50–55 (1996).
6. Yu, F., Morin, X., Cai, Y., Yang, X. & Chia, W. Analysis of partner of inscuteable, a novel player of Drosophila asymmetric divisions, reveals two distinct steps in inscuteable apical localization. *Cell* **100,** 399–409 (2000).
7. Siller, K. H., Cabernard, C. & Doe, C. Q. The NuMA-related Mud protein binds Pins and regulates spindle orientation in Drosophila neuroblasts. *Nat Cell Biol* **8,** 594–600 (2006).
8. Bowman, S. K., Neumüller, R. A., Novatchkova, M., Du, Q. & Knoblich, J. A. The Drosophila NuMA Homolog Mud regulates spindle orientation in asymmetric cell division. *Dev Cell* **10,** 731–742 (2006).
9. Izumi, Y., Ohta, N., Hisata, K., Raabe, T. & Matsuzaki, F. Drosophila Pins-binding protein Mud regulates spindle-polarity coupling and centrosome organization. *Nat Cell Biol* **8,** 586–593 (2006).
10. Guilgur, L. G., Prudencio, P., Ferreira, T., Pimenta-Marques, A. R. & Martinho, R. G. Drosophila aPKC is required for mitotic spindle orientation during symmetric division of epithelial cells. *Development* **139,** 503–513 (2012).
11. Nakajima, Y.-I., Meyer, E. J., Kroesen, A., McKinney, S. A. & Gibson, M. C. Epithelial junctions maintain tissue architecture by directing planar spindle orientation. *Nature* **500,** 359–362 (2013).
12. Packard, A. *et al.* Luminal mitosis drives epithelial cell dispersal within the branching ureteric bud. *Dev Cell* **27,** 319–330 (2013).
13. Ciruna, B., Jenny, A., Lee, D., Mlodzik, M. & Schier, A. F. Planar cell polarity signalling couples cell division and morphogenesis during neurulation. *Nature* **439,** 220–224 (2006).
14. Egger, B., Boone, J. Q., Stevens, N. R., Brand, A. H. & Doe, C. Q. Regulation of spindle orientation and neural stem cell fate in the Drosophila optic lobe. *Neural Dev* **2,** 1 (2007).
15. Rujano, M. A., Sanchez-Pulido, L., Pennetier, C., le Dez, G. & Basto, R. The microcephaly protein Asp regulates neuroepithelium morphogenesis by controlling the spatial distribution of myosin II. *Nat Cell Biol* **15,** 1294–1306 (2013).

16. Herszterg, S., Leibfried, A., Bosveld, F., Martin, C. & Bellaïche, Y. Interplay between the Dividing Cell and Its Neighbors Regulates Adherens Junction Formation during Cytokinesis in Epithelial Tissue. *Dev Cell* **24,** 256–270 (2013).
17. Morais-de-Sá, E. & Sunkel, C. Adherens junctions determine the apical position of the midbody during follicular epithelial cell division. *EMBO Rep.* **14,** 696–703 (2013).
18. Tanentzapf, G., Smith, C., McGlade, J. & Tepass, U. Apical, lateral, and basal polarization cues contribute to the development of the follicular epithelium during Drosophila oogenesis. *J Cell Biol* **151,** 891–904 (2000).
19. Bieber, A. J. *et al.* Drosophila neuroglian: A member of the immunoglobulin superfamily with extensive homology to the vertebrate neural adhesion molecule L1. *Cell* **59,** 447–460 (1989).
20. Grenningloh, G., Rehm, E. J. & Goodman, C. S. Genetic analysis of growth cone guidance in Drosophila: fasciclin II functions as a neuronal recognition molecule. *Cell* **67,** 45–57 (1991).
21. Szafranski, P. & Goode, S. A Fasciclin 2 morphogenetic switch organizes epithelial cell cluster polarity and motility. *Development* **131,** 2023–2036 (2004).
22. Wei, J., Hortsch, M. & Goode, S. Neuroglian stabilizes epithelial structure during Drosophila oogenesis. *Dev. Dyn.* **230,** 800–808 (2004).
23. Szafranski, P. & Goode, S. Basolateral junctions are sufficient to suppress epithelial invasion during Drosophila oogenesis. *Dev. Dyn.* **236,** 364–373 (2007).
24. Bilder, D. Epithelial polarity and proliferation control: links from the Drosophila neoplastic tumor suppressors. *Genes Dev* **18,** 1909–1925 (2004).
25. Lecuit, T. & Lenne, P.-F. Cell surface mechanics and the control of cell shape, tissue patterns and morphogenesis. *Nat. Rev. Mol. Cell Biol.* **8,** 633–644 (2007).
26. Genova, J. L. & Fehon, R. G. Neuroglian, Gliotactin, and the Na+/K+ ATPase are essential for septate junction function in Drosophila. *Journal of Cell Biology* **161,** 979–989 (2003).
27. Besse, F. & Pret, A.-M. Apoptosis-mediated cell death within the ovarian polar cell lineage of Drosophila melanogaster. *Development* **130,** 1017–1027 (2003).

Acknowledgments:

The authors are grateful to Ross Nieuwburg, the St Johnston group, and other Gurdon Institute members for suggestions. We thank the Bloomington Stock Center, J. Knoblich, and the TRiP at Harvard Medical School (NIH/NIGMS R01-GM084947) for fly stocks. We thank Nick Lowe for technical assistance. This work was supported by a Wellcome Trust Principal Fellowship to DStJ [080007], and by core support from the Wellcome Trust [092096] and Cancer Research UK [A14492]. DTB was supported by a Marie Curie Fellowship and the Wellcome Trust. HEL was supported by a Herchel Smith Studentship.

Author Contributions:

DTB and HEL performed the experiments and data analysis. DTB, HEL, and DStJ planned the experiments. DTB and DStJ conceived the project and wrote the manuscript.

Competing Financial Interest

The authors declare no competing financial interests.

Figure Legends

Fig. 1

Spindle misorientation does not disrupt the organisation of the follicle epithelium

A) The organisation of the follicle cells into an epithelial monolayer is normal in *mud*^{3}/*mud*^{4} transheterozygotes. Disorganization was not observed in any of 42 ovarioles imaged.
B) Incorrectly oriented divisions are observed in *mud* mutant egg chambers. Five such complete reorientations were observed. These are exceptional cases, given that *mud* mutation randomizes, rather that perpendicularizes, divisions.
C) Ectopically expressed Inscuteable localizes apically and causes spindle reorientation in follicle cells. This image is one of the 20 divisions quantified in Figure 1D.
D) A cumulative data plot of spindle angles in wild type (n = 29 spindles assessed from 29 different egg chambers) and UAS-Inscuteable expressing (n = 20 spindles assessed from 20 different egg chambers) follicle cells shows the extent of spindle misorientation caused by Inscuteable expression. $p = 1.047\text{x}10^{-10}$ as determined by the Kolmogorov-Smirnof test.
E) Inscuteable expression does not disrupt the organisation of the follicular epithelium. This image is representative of 103 ovarioles imaged.
F) The apical product of a misoriented division reintegrates into the monolayer. Clonal expression of Actin-Gal4 was used to drive both UAS-Inscuteable and UAS-GFP, which illuminates the relevant cell (arrow) and its neighbors to the left. Tubulin-RFP marks the misoriented spindle at time -5'. As in subsequent timelapses, the 0' timepoint represents abscission. This is one of seven complete reintegrations imaged.
Scale bars in this figure represent 10μM.

Fig. 2

Reintegration is a feature of wild type cell division in the follicle epithelium.

A and B) During division cells usually move apically relative to the epithelial layer, often appearing to detach detaching from the basement membrane (Viking-GFP). One prometaphase cell is shown in (A) and two recently born sister cells in (B). These fixed-tissue images are representative of the live divisions quantified in (C).
C) Cells are frequently born without an obvious connection to the basement membrane. Divisions were imaged live to a depth of at least 10 microns to confirm the position of each cell in the tissue. *n* = number of cell divisions.
D) Reintegration occurs in wild type tissue. Egg chambers were imaged live using Jupiter:Cherry to mark the spindle and Basigin-YFP to mark the cell outline. Images taken from Supplementary Movie 2. Timepoints in this and all subsequent timecourses are numbered relative to abcission (at zero). This movie is one of the 60 divisions quantified in C.
Scale bars in this figure represent 10μM.

Fig. 3

Reintegration occurs in multiple epithelia

A) Inscuteable expression causes spindle misorientation in the optic lobe neuroepithelium. The two daughter cells are tracked in (C). This image is representative of the Inscuteable-induced spindle misorientation in this tissue quantified in Egger et al[14].
B) Expression of Inscuteable reorients mitotic spindles in the early embryonic ectoderm. Spindles are perpendicular to the plane of the epithelium. These spindles are among the 34 quantified in Supplemental Figure 3B.
C) Both products of a misoriented division are maintained in the neuroepithelial layer. Pseudo-colouring indicates the two division products. By the 12' minute timepoint, the basal daughter has reattached to the apical surface. After this point it moves orthogonally to the plane of focus and is no longer observed. This is one of two complete reintegrations imaged in this tissue.

D) Reintegration of two basally misplaced cells following misoriented divisions in the embryonic ectoderm. Arrows point to correctly positioned daughter cells. The basally mispositioned daughters are marked by asterisks. These reintegrations, representing two of the three tracked, were exceptional; other misplaced daughter cells could not be tracked due to the rapid morphogenetic movements of the tissue and the limited depth resolution.

Scale bars in this figure represent 10μM.

Fig. 4

Reintegration occurs despite weakened adherens junctions

A) Reintegration is characterized by by an apical protrusion as the basal side of the cell reintegrates. Only one of two division products (marked by an asterisk) is seen in this plane of focus. This movie is representative of the 60 divisions quantified in Figure 2C.

B) Localized cortical enrichment of Sqh is not observed during reintegration. Arrows point to Sqh enrichment at the contractile ring. The reintegrating cell is marked with an asterisk. This represents one of 20 divisions imaged using these markers.

C) The apical product of a misoriented division remains attached to the epithelial layer via adherens junctions. This is one of three similar images collected.

D) Following an Inscuteable-induced perpendicular division, the basal daughter cell establishes a transient adherens junction along the length of its lateral cortex (marked by Armadillo-GFP) with the neighboring cell. Two Z-planes spaced 1μm apart were merged. This is one of two complete divisions imaged with these markers.

E) Overexpression of Inscuteable (marked by co-expression of UAS-GFP) in *armadillo*^{3} mutant clones (marked by loss of RFP) does not promote multilayering. This image is one of the 15 clones of > 5 cells, none of which showed multilayering.

Scale bars in this figure represent 10μM.

Fig. 5

Reintegration is driven by lateral cell-cell adhesion

A) Neuroglian expression in follicle cells is higher in mitotic stage egg chambers than in post-mitotic stages. This image is representative of 16.

B) Fas2 expression decreases after mitotic stages. This image is representative of 18.

C and D) Neuroglian knockdown (C) or *Fas2* mutation (D) leads to occassional follicle cells that lie apical to the monolayer. These egg chambers, quantified in Figure 5H, represent 1 of 12 (Nrg-shRNA) and 1 of 15 (*Fas2* mutant clones).

E and F) Co-expression of Inscuteable with Nrg-RNAi (E) or expression of Inscuteable in $Fas2^{G0336}$ mutant clones (F) increases the number of follicle cells above the epithelial monolayer. These egg chambers, quantified in Figure 5H, represent 1 of 17 (Nrg-shRNA) and 1 of 10 ($Fas2^{G0336}$ clones).

G) Misplaced cells are a consequence of failed reintegrations. A timecourse of 60 minutes shows a cell that fails to reintegrate (marked with an asterisk). This is one of 4 such divisions imaged.

H) Quantification of the frequency of misplaced cells. For Nrg-shRNA, $n = 12$ (control) or 17 (Inscuteable expression) stage 6 egg chambers. $p = 0.0091$ (*). For $Fas2^{G0336}$ clones, $n = 15$ (control) or 10 (Inscuteable expression) stage 6 egg chambers over 50% RFP negative ($Fas2^{G0336}/Fas2^{G0336}$). $p = 0.0014$ (**). Significance was determined using an unpaired, two-tailed students t-test with Welch's correction. Boxes represent the interquartile range (IQR). Whiskers extend from the lowest point within 1.5 IQR of the lower quartile to the highest point within 1.5 IQR of the upper quartile. The center line is the median.

I) A model illustrating the "zipping-up" of lateral adhesion molecules to drive cell reintegration. Although neighboring cells must unzip, adhesion at the tissue level is increased by the integration of an additional cell.

Scale bars in this figure represent 10μM.

Methods

Mutant alleles: The following *Drosophila melanogaster* mutant alleles have been described previously and can be referenced on FlyBase.org: *armadillo*[3], *mud*[3] and *mud*[2], and *pins*[p62]. *Fas2*[G0336] was obtained from the Bloomington Drosophila Stock Center.

Fluorescent marker stocks: Neuroglian::YFP, Zipper::YFP, and Basigin::YFP are Cambridge Protein Trap Insertion lines. Jupiter::Cherry was derived by Nick Lowe from the Jupiter::YFP CPTI line using P-element exchange. Bazooka::GFP was generated by the Carnegie Protein Trap Project. The following markers have been described previously: Viking-GFP[28], Arm-GFP[29], pUbq-α-Tub-RFP[30], Sqh-mCherry[31], and Histone 2B-RFP[32].

GAL4 drivers: Ectopic protein expression was accomplished using the UAS-GAL4 system. Expression in follicle cells was induced by any of the following drivers: T155-Gal4, GR1-Gal4, Traffic Jam-Gal4, or actin5c-FLPout-Gal4 (inducible by FRT/FLP mediated removal of a stop codon). Expression in the larval optic lobe was driven using c855a-Gal4. Expression in the embryo was driven with matα4-GAL4:VP16.

UAS lines: The UAS-Neuroglian-shRNA line TRiP.HMS01638 was generated by the Transgenic RNAi Research Project. UAS-Inscuteable[33] and UAS-p35[34] have been described previously.

Reagents: The following antibodies were used in this study: mouse anti-Armadillo (N2 7A1), anti-Fas2 (1D4), and anti-Discs large (4F3) (Developmental Studies Hybridoma Bank), rabbit anti-aPKC (sc216), mouse anti-α-tubulin (F2168) (Sigma), rabbit anti-cleaved Caspase-3 (8G10 #9665) (Cell Signaling), rabbit anti-Inscuteable[33] and rabbit anti-Par6[35] (gifts from Jürgen Knoblich), rabbit anti-Scribble[36] and rat anti-Deadpan[37] (gift from Chris Doe), di-phospho Sqh[38] (gift from Robert Ward), rat anti-DE Cadherin[39] (gift from Hiroki Oda), and rabbit anti-Bazooka[40] (gift from A. Wodarz). Rhodamine-Phalloidin was purchased from Invitrogen. Vectashield with DAPI was purchased from Vector Labs. Conjugated secondary antibodies were purchased from Jackson Immunoresearch. CellMask was purchased from Life Technologies.

Immunostaining: Ovaries were fixed for 10 minutes in 10% Paraformaldehyde and 2% Tween in Phosphate Buffered Saline. Ovaries were then incubated in 10% Bovine Serum

Albumin (in PBS) to block for one hour at room temperature. Embryos were dechorionated with 50% bleach for 3-5 minutes, then washed three times with water. Embryos were fixed for 20 minutes in 6% Paraformaldehyde in PBS overlayed with heptane (1:1 fixative:heptane). To divitellinize the embryos, the lower phase was removed and replaced with methanol. After vigorously shaking the vial for 30 seconds, divitellinized embryos sank down from the interphase into the lower phase. These embryos were washed three times in PBS with 0.2% Tween. For both ovaries and embryos the primary and secondary immunostainings lasted at least 3 hours in PBS with 0.2% Tween. Three washes (approximately 10 minutes each) in PBS-0.2% Tween were carried out between stainings and after the secondary staining. Primary antibodies were diluted 1:150. Secondary antibodies and phalloidin were diluted 1:1000.

Imaging: Fixed cell imaging was performed using an Olympus IX81 (40x/1.3 UPlan FLN Oil or 60x/1.35 UPlanSApo Oil). Live imaging was performed using a Leica SP5 (63x/1.4 HCX PL Apo CS Oil) or Olympus IX81 (40x/1.3 UPlan FLN Oil or 60x/1.35 UPlanSApo Oil) inverted, used with or without a Yokogawa CSU22 spinning disc imaging system. Ovaries were dissected and imaged in Schneider's Medium (Sigma) with 10mg/ml insulin (Sigma) and 0.2% agarose or in 10S Voltalef Oil (VWR). Embryos were imaged in 10S Voltalef. Optic lobes were imaged in Schneider's with insulin and agarose. Images were collected with Olympus Fluoview Ver 3.1, MetaMorph software, or Leica LAS AF and processed (Gaussian blur) using Image J. In Fig. 2C, each timepoint represents a Z-projection of three slices spaced 1 μm apart. In Fig. 2D, each timepoint represents a Z-projection of five slices spaced 2 μm apart.

Spindle angle measurements: Spindle angles were calculated using Image J. The angle was measured between one line drawn connecting the apical corners of the mitotic cell and another line drawn along the spindle.

Statistical analyses: The Kolmogorov-Smirnov test was used to determine significance between metaphase spindle angles. An unpaired, two-tailed students t-test with Welch's correction was used to determine significance when comparing the number of misplaced cells in an egg chamber. No statistical method was used to predetermine sample size, the experiments were not randomized, and the investigators were not blinded to allocation during experiments and outcome assessment.

Box plots: Box plots were generated using BoxPlotR. The position of whiskers was determined by the Tukey method.

Misplaced cell counting: Ten Stage 6 egg chambers from six flies were counted in each condition. The phenotype of *Fas2*^{G0336} mutant egg chambers was measured in only those egg chambers that were at least 50% mutant.

***Drosophila* genetics:** Follicle cell clones of *pins*^{p62}, *Fas2*^{G0336}, and *arm*^{3} were induced by incubating larvae or pupae at 37° for two out of every twelve hours over a period of at least two days. Adult females were dissected at least two days after the last heat shock. In two *arm*^{3} mutant clones, we observed one cell apical to the layer. These cells had condensed nuclei, indicating that they were newly born and had yet to reintegrate.

Reproducibility of Experiments: Images represent the number of independent experiments as follows: Figure 1A (42), 1B (5), 1C (20), 1E (103), 1F (7). Figures 2A, 2B, and 2D are representative of the 60 live divisions quantified in 2C. Figure 3B (34), 3C (2), 3D (2 of 3). Figure 4A (60), 4B (20), 4C (3), 4D (2), 4E (15). Figure 5A (16), 5B (18), 5C (12), 5D (15), 5E (17), 5F (10), 5G (4). Supplementary Figure 1A (83), 1B (7), 1C (6), 1D (4), 1F (23), 1G (12). Supplementary Figure 2A (5), 2B (11), 2C (14). Supplementary Figure 3A (2) and 3D (3). Supplementary Figure 4A (9), 4B (7), 4C (3), 4D (2). Supplementary Figure 5A (5), 5B (8), 5C (9), 5D (7), 5E (5), 5F (6), 5G (4), 5H (6), 5I (5), 5J (3). Figures 3A, Supplementary Figure 3C, and Supplementary Figure 1E are representative of previously published work and included in this manuscript for confirmation and comparison[5,14,27].

Method References

28. Morin, X., Daneman, R., Zavortink, M. & Chia, W. A protein trap strategy to detect GFP-tagged proteins expressed from their endogenous loci in Drosophila. *Proc Natl Acad Sci USA* **98,** 15050–15055 (2001).
29. McCartney, B. M. *et al.* Drosophila APC2 and Armadillo participate in tethering mitotic spindles to cortical actin. *Nat Cell Biol* **3,** 933–938 (2001).
30. Basto, R. *et al.* Centrosome amplification can initiate tumorigenesis in flies. *Cell* **133,** 1032–1042 (2008).
31. Martin, A. C., Kaschube, M. & Wieschaus, E. F. Pulsed contractions of an actin-myosin network drive apical constriction. *Nature* **457,** 495–499 (2009).
32. Pandey, R., Heidmann, S. & Lehner, C. F. Epithelial re-organization and dynamics of progression through mitosis in Drosophila separase complex mutants. *J Cell Sci* (2005).
33. Kraut, R., Chia, W., Jan, L. Y., Jan, Y. N. & Knoblich, J. A. Role of inscuteable in orienting asymmetric cell divisions in Drosophila. *Nature* **383,** 50–55 (1996).
34. Zhou, L. *et al.* Cooperative functions of the reaper and head involution defective genes in the programmed cell death of Drosophila central nervous system midline cells. *Proc Natl Acad Sci USA* **94,** 5131–5136 (1997).
35. Petronczki, M. & Knoblich, J. A. DmPAR-6 directs epithelial polarity and asymmetric cell division of neuroblasts in Drosophila. *Nat Cell Biol* **3,** 43–49 (2001).
36. Albertson, R. & Doe, C. Q. Dlg, Scrib and Lgl regulate neuroblast cell size and mitotic spindle asymmetry. *Nat Cell Biol* **5,** 166–170 (2003).
37. Lee, C.-Y., Robinson, K. J. & Doe, C. Q. Lgl, Pins and aPKC regulate neuroblast self-renewal versus differentiation. *Nature* **439,** 594–598 (2006).
38. Zhang, L. & Ward, R. E. Distinct tissue distributions and subcellular localizations of differently phosphorylated forms of the myosin regulatory light chain in Drosophila. *Gene Expr. Patterns* **11,** 93–104 (2011).
39. Oda, H., Uemura, T., Harada, Y., Iwai, Y. & Takeichi, M. A Drosophila homolog of cadherin associated with armadillo and essential for embryonic cell-cell adhesion. *Developmental Biology* **165,** 716–726 (1994).
40. Wodarz, A., Ramrath, A., Kuchinke, U. & Knust, E. Bazooka provides an apical cue for Inscuteable localization in Drosophila neuroblasts. *Nature* **402,** 544–547 (1999).

Supplementary Fig. 1

Neither mutation of Pins nor overexpression of Inscuteable cause disorganization of the follicle epithelium

A) Loss of Pins function does not affect the organization of the follicle cell monolayer. *pins*^{p62} mutant clones are marked by the absence of GFP. This is one of 83 ovarioles imaged.

B) Inscuteable expression promotes reorientation of cell division. The circled division is in early telophase, with the two daughters connected by a thick, central midbody. This is one of seven completely reoriented divisions imaged.

C) UAS-GFP is a reliable marker for Inscuteable expression. For the experiment in Fig. 1E we used the FLPout system to express UAS-Inscuteable and UAS-GFP in large clonal populations. The sample in Fig. 1E was also stained for Inscuteable, which is shown here in red. GFP is not always a reliable marker in the follicle epithelium as it can leak between sister follicle cells through somatic ring canals. However, immunoreactivity with the anti-Inscuteable antibodies overlaps substantially with the expression of UAS-GFP. This result was confirmed in six ovarioles imaged. This result show that UAS-GFP is a reliable marker for Inscuteable expression in Fig. 1F and Supplementary Video 1.

D) Inscuteable expressing follicle cells do not express the neuroblast marker Deadpan. Traffic-Jam Gal4 was used to drive both UAS-Inscuteable and UAS-myr.RFP in the follicle epithelium. The Deadpan antisera gives a non-specific background signal (D') that is not due to Deadpan protein as it is extends into the germline, is not nuclear, and does not correlate with myr.RFP intensity (D).

E) Neither product of a misoriented division is apoptotic. This is one image representative of 13. A supernumerary polar cell provides a positive control for caspase-3 immunoreactivity. This was shown previously[27].

F) Co-expression of p35 with UAS-Inscuteable does not cause tumor formation. This image is representative of 23 Stage 4-6 egg chambers.

G) Expression of p35 in *pins*^{p62} mutant clones (cells lacking GFP) does not cause tumor formation. This image is representative of 12 clones < 5 cells in Stage 4-6 egg chambers. Scale bars in this figure represent 10μM.

Supplementary Fig. 2

Follicle cells move relative to the layer during division

A) An early stage egg chamber, imaged live, has an uneven appearance. The plasma membrane is stained with Cell Mask. This uneveness was consistently observed in over two hundred live imaging experiments using a variety of markers. This particular staining (Cell Mask alone) was performed five times.
B) Mitotic cell rounding is accompanied by an increase in di-phosphorylated (active) myosin regulatory light chain (Spaghetti Squash). This is one image representative of 11.
C) Detachment of a new daughter cell from the basement membrane (in box) is confirmed by three dimensional imaging. The lateral marker Discs large extends fully around the basal cortex of the daughter cell. Images are 20 planes spaced .5 μm apart, collapsed to show the full diameter of the cell in all dimensions. This is one image representative of 14.
Scale bars in this figure represent 10μM.

Supplementary Fig. 3

Reintegration occurs in the embryo and optic lobe

A) Reintegration in the neuroepithelium of the optic lobe. These data are also presented in Fig. 3C with false coloring to indicate division products. This is one of two complete reintegrations imaged.
B) Quantification of Domain 11 spindle angles in wild type (n = 33 cells) or embryos expressing Inscuteable (n = 34 cells). The distribution of angles differs significantly, with

a *p* value of 1.618×10^{-12} as determined by the Kolmogorov-Smirnov test. Spindle angles are presented as a cumulative data plot.

C) A transverse image of an embryo at approximately Stage 8 of development shows exogenously expressed Inscuteable (in red) localized apically. A dividing epithelial cell at telophase (within the white outline) is oriented along the apical-basal axis. This is representative of previous work published by Kraut *et al*[5].

D) The basal product of a misoriented division in the early embryo reintegrates apically into the layer. The cell is followed in both XY and YZ planes. The dashed grey line in the first image of the YZ plane (top left) indicates the plane of focus in the XY images below. The white arrows in the YZ planes (top) point to the basal daughter cell. The arrow in the XY plane at 3' points to the first appearance of the reintegrating cell in the plane of focus. This "hole" in the layer does not become obvious again until 6', when the nucelus of the reintegrating cell moves into the focal plane.

Scale bars in this figure represent 10μM.

Supplementary Fig. 4

Cell reintegration does not depend on myosin or adherens junctions

A) Zipper::YFP does not show localized cortical enrichment apically or basally in a dividing cell detached from the basement membrane. The arrow points to enrichment at the contractile ring. The egg chamber was imaged live. This is one of nine divisions imaged with these markers.

B) A reintegrating cell can demonstrate expansion at its apical cortex. The egg chamber was imaged live using Basigin::YFP to mark cell outlines. This is one of seven such expansions observed.

C) The apical daughter cell of an Inscuteable-induced perpendicular division inherits the adherens junction belt (large arrows). A new adherens junction is also made between sister cells (small arrow). Gal4 activity marked with UAS-myristoylated.RFP. This is one image representative of three.

D) Live imaging shows that an *arm*^{3} mutant cell can reintegrate. Mutant cells are marked by the absence of GFP. Cell outlines were marked with CellMask. This is one of two complete reintegrations imaged.
Scale bars in this figure represent 10μM.

Supplementary Fig. 5

Neuroglian and Fas2 are required for reintegration but not polarity

A) Neuroglian is expressed at lateral cell-cell contacting surfaces in the embryonic ectoderm at approximately Stage 8 of development. A' is a Z-reconstruction of images taken 0.5μM apart. This is one image representative of 5.
B) Neuroglian is expressed along the lateral cortex of cells in the developing neuroepithelium. This is one image representative of eight.
C) *Fas2*^{G0336} clones are Fas2 protein null as measured by antibody staining. This is one image representative of nine.
D and E) Epithelial cell polarity is unaffected by the *Fas2* mutation (D) or Nrg-RNAi (E), as revealed by staining for the polarity markers aPKC (apical - red) and Discs large (lateral - green). Wild type cells in (D) are marked by the absence of RFP (in gray). These images represent one of seven (D) or five (E).
F-I) Loss of Nrg does not alter that expression of factors that influence adhesion at the level of adherens junctions. Actin-Gal4 drives clonal expression of GFP and Nrg shRNAi. Egg chambers were stained for F) DE-Cadherin, G) Armadillo, H) Par-6, and I) Bazooka. These images represent one of six (F), four (G), six (H), and five (I).
J) A series of still images showing the failure of a cell expressing both Nrg-shRNA and Inscuteable to reintegrate in follicle epithelium. The cell was observed for 80 minutes total. Cell outlines were marked with CellMask. This is one of three such failed reintegrations imaged.
Scale bars in this figure represent 10μM.

Supplementary Movie 1

Reintegration of a follicle cell after a misoriented division

GFP marks cells expressing Inscuteable. Tubulin-RFP marks the mitotic spindle. Frames taken one minute apart. The frame rate is seven per second. Each frame is a merge of 4 planes spaced 1μM apart. The scale bar represents 10μM.

Supplementary Movie 2

Reintegration in wild type follicle epithelium

Cells marked with Basigin::YFP to reveal cell outlines and Jupiter-Cherry to reveal the mitotic spindle. Each frame is a merge of four planes spaced 1μM apart. Frames taken one minute apart. The frame rate is seven per second. The scale bar represents 10μM.

Supplementary Movie 3

Reintegration in the neuroepithelium of the optic lobe

Inscuteable expression was induced to misorient spindles and divisions. Cell outlines were marked with Basigin::YFP. Each frame represents a Z-projection of three slices spaced one μm apart. The apical division product is marked with a red asterisk. After reaching the bottom of the tissue the cell again moves up and divides. Frames are two minutes apart. The frame rate is five per second. The scale bar represents 10μM.

Supplementary Movie 4

A wild type follicle cell expands its apical surface as it reintegrates into the monolayer

The other division product is not visible in this plane of focus. Cell outlines marked with CellMask. Frames taken one minute apart. The frame rate is seven per second. The scale bar represents 10μM.

Supplementary Movie 5

Myosin Regulatory Light Chain is not asymmetrically localized in a wild type reintegrating follicle cell

Myosin is labelled with Sqh-RFP. Cell outlines are marked with Basigin-YFP. Frames taken one minute apart. The frame rate is seven per second. The scale bar represents 10μM.

Supplementary Movie 6

A transient adherens junction is made by the basal daughter cell of a misoriented division

UAS-Inscuteable expression was driven with Traffic-Jam Gal4. Frames were taken one minute apart. The frame rate is seven per second. Note that the apical daughter cell moves backwards out of the plane of focus as it reintegrates. The scale bar represents 10μM.

Supplementary Movie 7

Nrg localizes along the cortex during reintegration

Nrg-YFP remains localized along the cortex during reintegration. Frames taken one minute apart. The frame rate is seven per second. This reintegration takes place in wild type tissue. The scale bar represents 10μM.

Supplementary Movie 8

A *Fas2*^{G0336} mutant follicle cell expressing Inscuteable fails to reintegrate

Mutant cells are marked by the absence of RFP in green. Cell outlines marked with CellMask. UAS-Inscuteable expression was driven with Traffic-Jam Gal4. Frames taken one minute apart. The frame rate is seven per second. The scale bar represents 10μM.

Figure 1

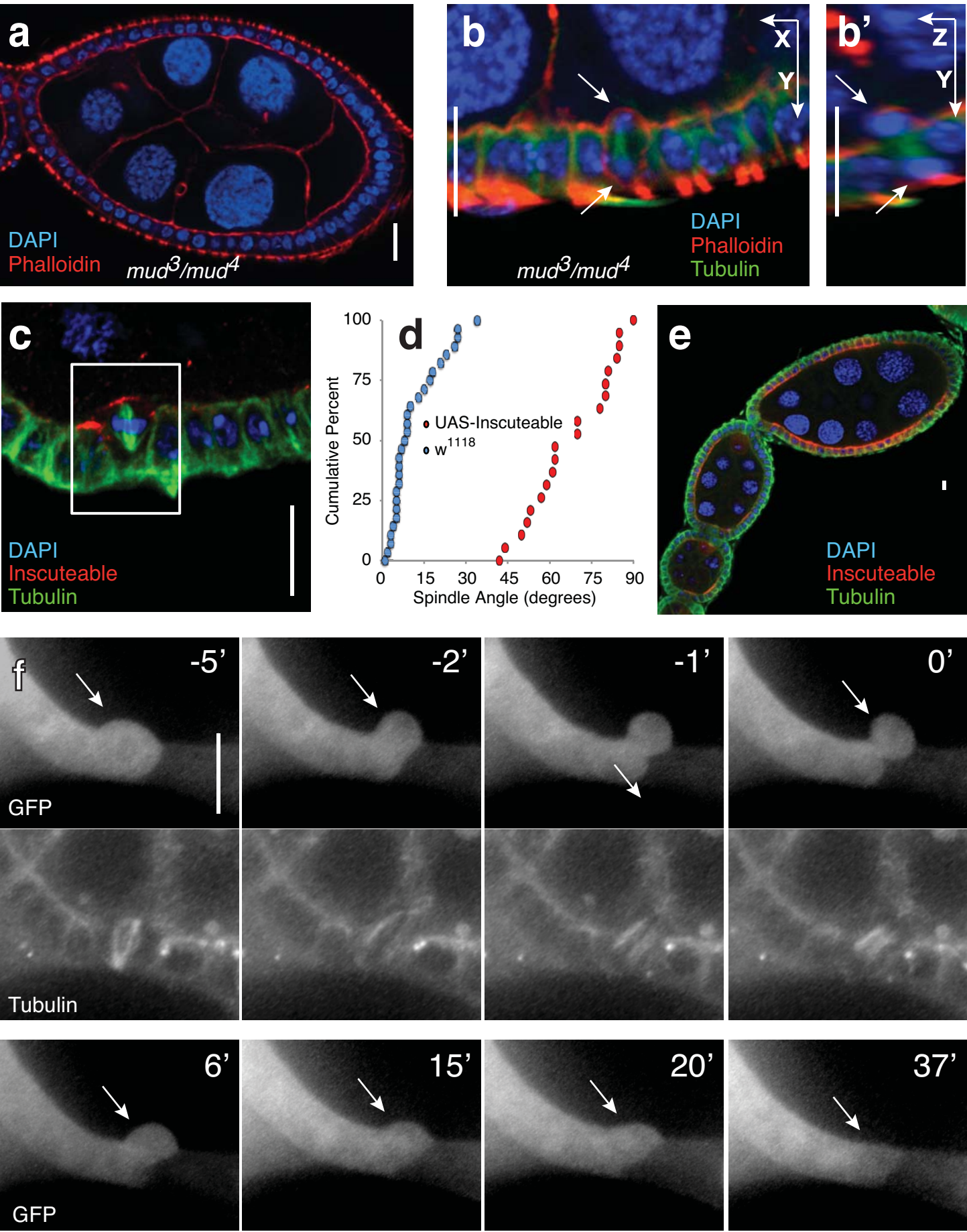
a
DAPI
Phalloidin
mud3/mud4
b
x
Y
DAPI
Phalloidin
Tubulin
mud3/mud4
b'
z
Y
c
DAPI
Inscuteable
Tubulin
d
Cumulative Percent
100
75
50
25
0
0
15
30
45
60
75
90
Spindle Angle (degrees)
UAS-Inscuteable
w1118
e
DAPI
Inscuteable
Tubulin
f
-5'
-2'
-1'
0'
GFP
Tubulin
6'
15'
20'
37'
GFP

Figure 2

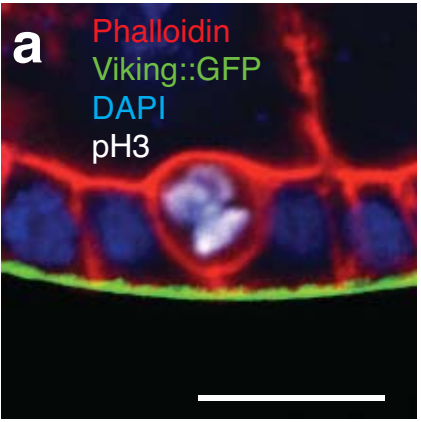

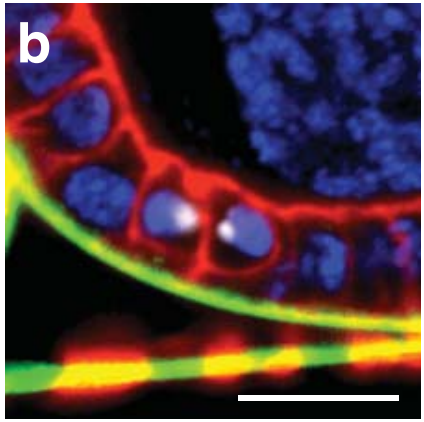

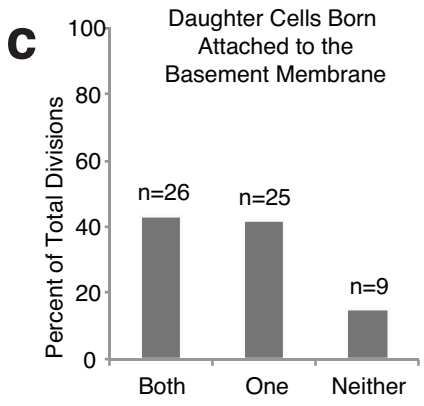

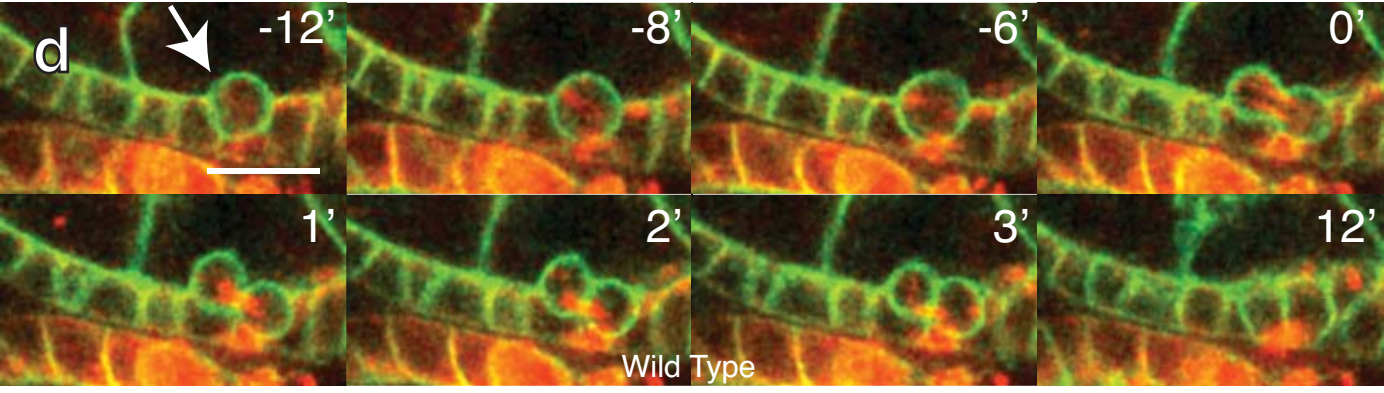

Jupiter::Cherry Basigin::YFP

Figure 3

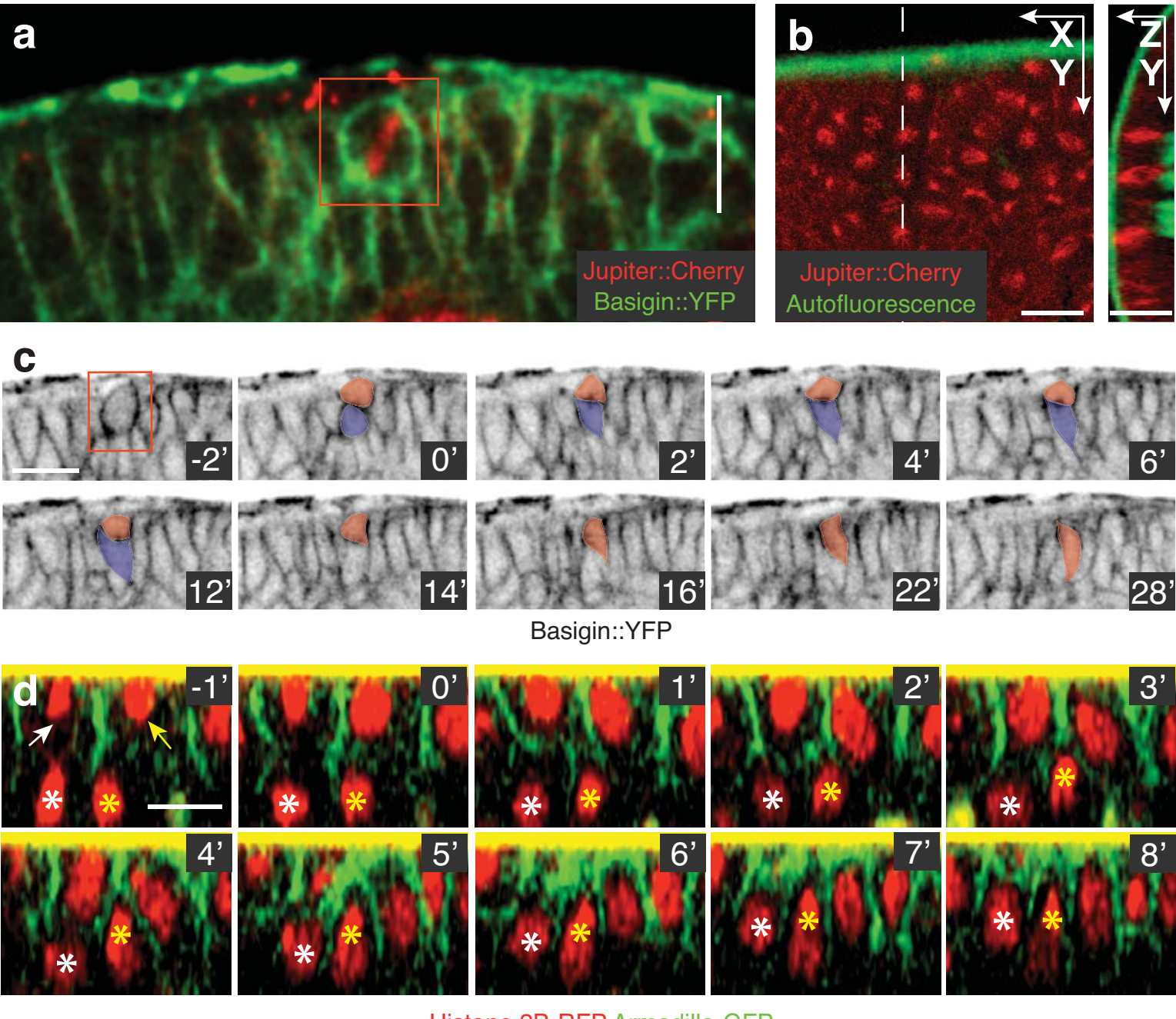
a
Jupiter::Cherry
Basigin::YFP
b
X
Y
Z
Y
Jupiter::Cherry
Autofluorescence
c
-2'
0'
2'
4'
6'
12'
14'
16'
22'
28'
Basigin::YFP
d
-1'
0'
1'
2'
3'
4'
5'
6'
7'
8'
Histone 2B-RFP Armadillo-GFP

Figure 4

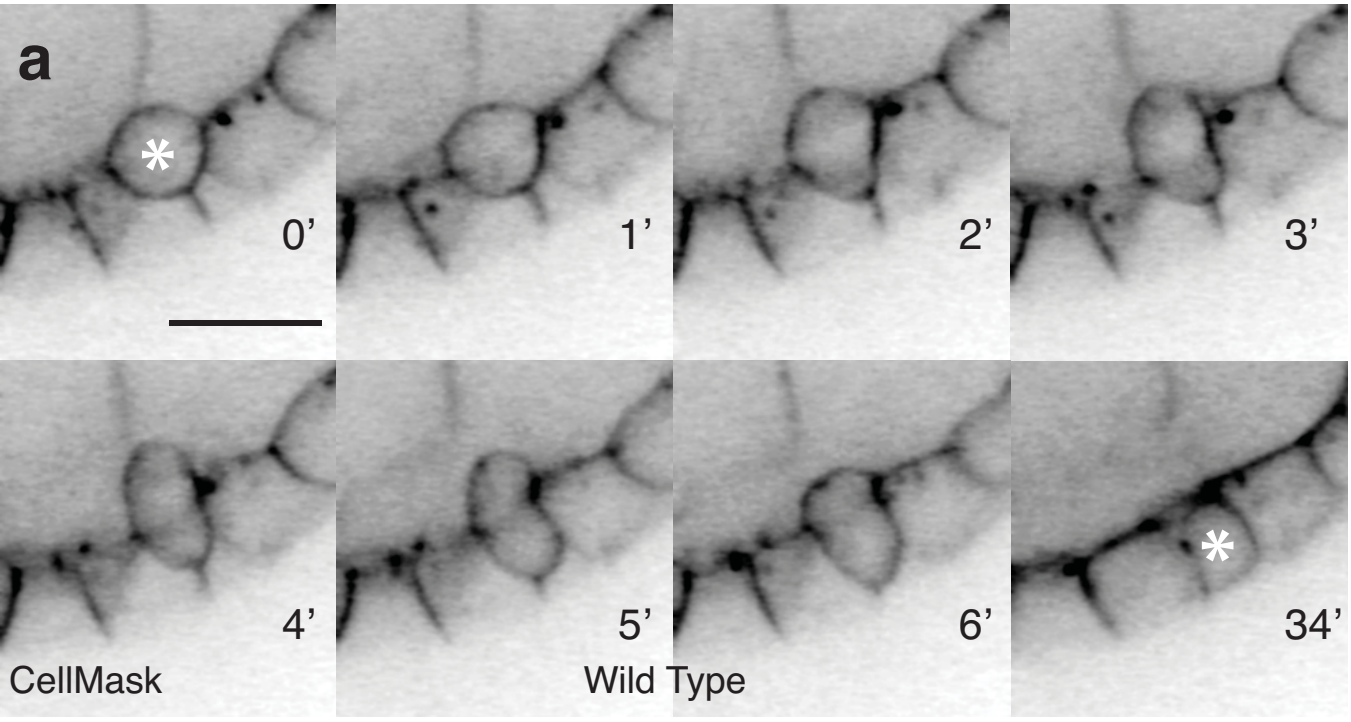
a
0’
1’
2’
3’
4’
5’
6’
34’
CellMask
Wild Type

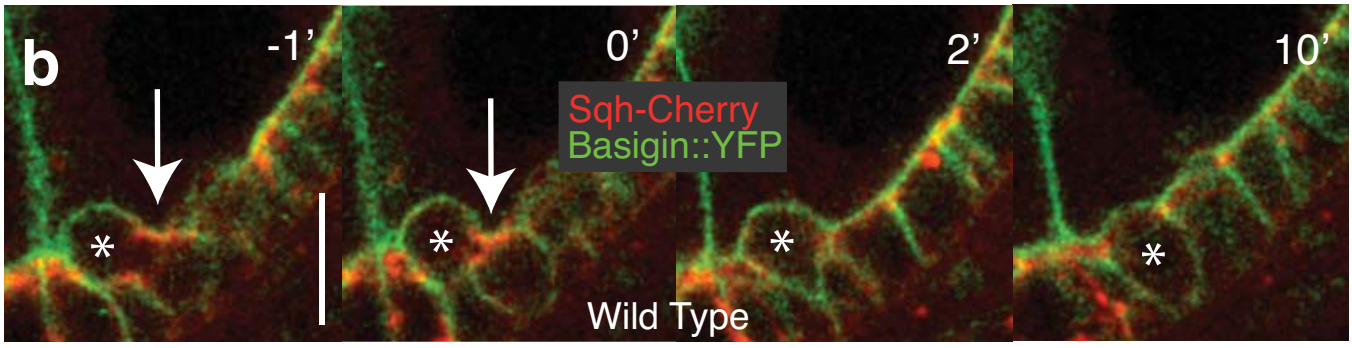
b
-1’
0’
2’
10’
Sqh-Cherry
Basigin::YFP
Wild Type

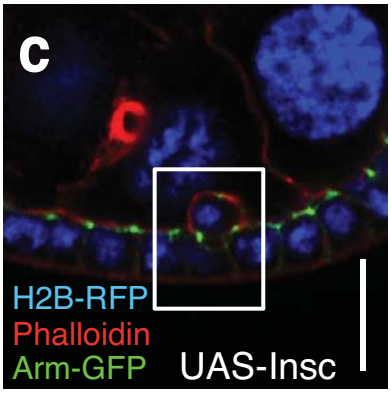
c
H2B-RFP
Phalloidin
Arm-GFP
UAS-Insc

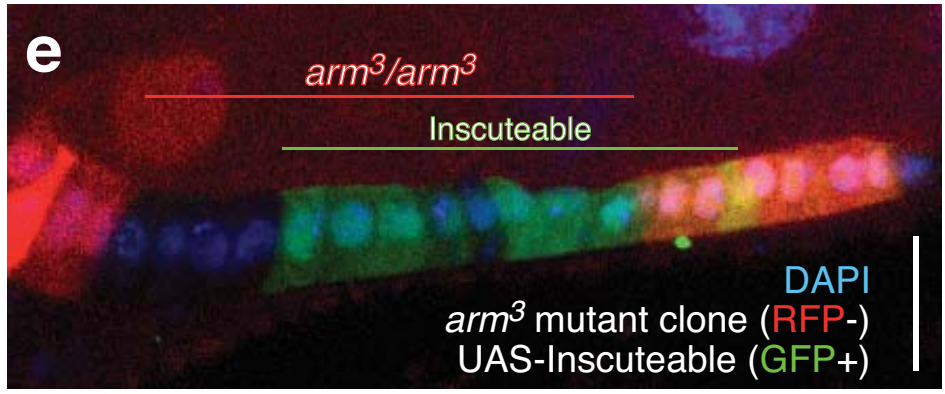
e
arm3/arm3
Inscuteable
DAPI
arm3 mutant clone (RFP-)
UAS-Inscuteable (GFP+)

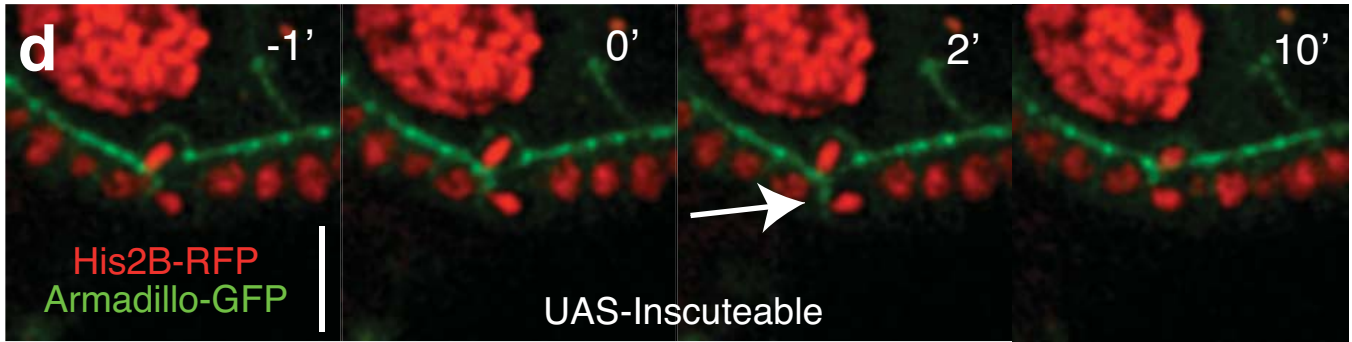
d
-1’
0’
2’
10’
His2B-RFP
Armadillo-GFP
UAS-Inscuteable

Figure 5

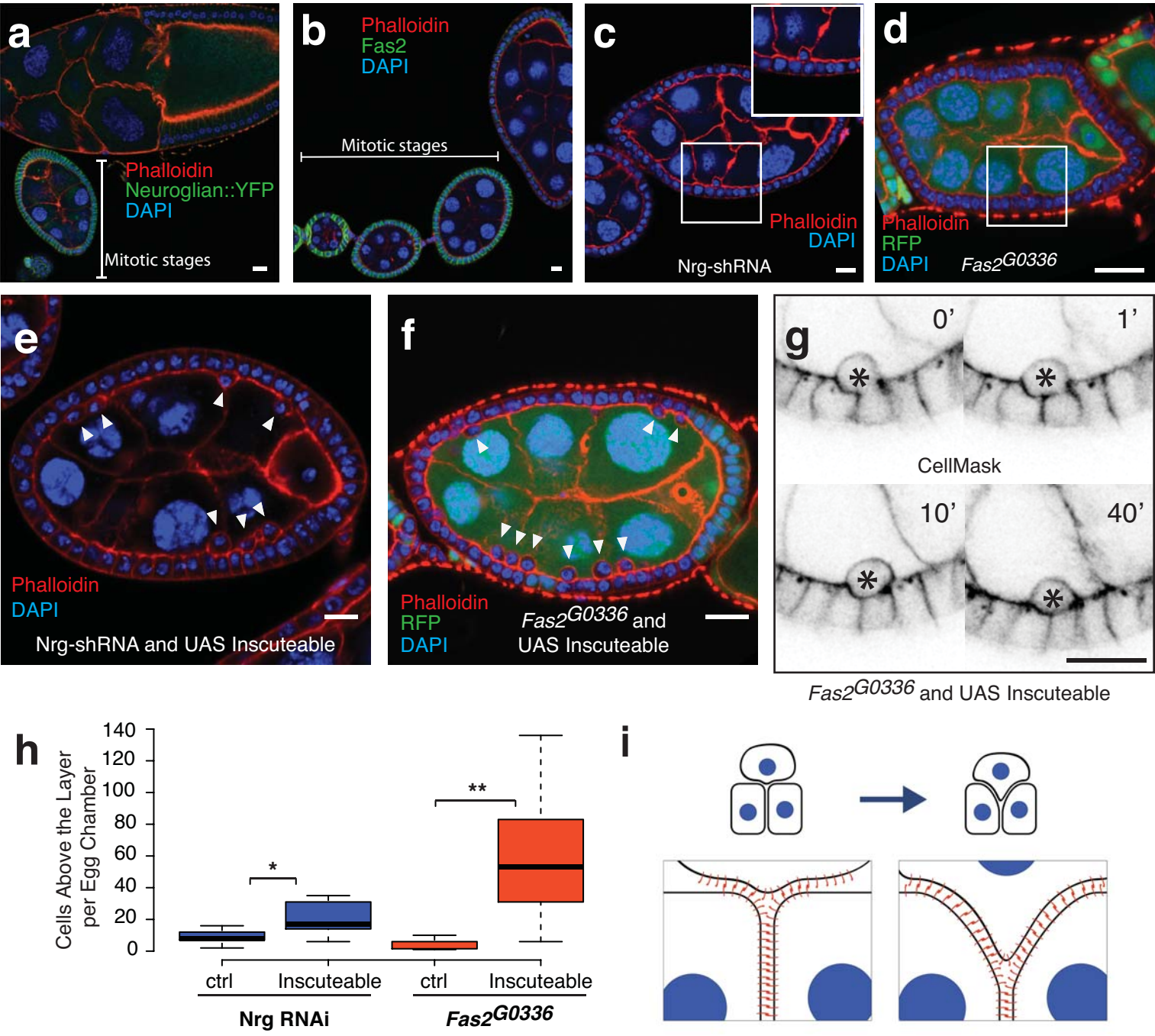
a
Phalloidin
Neuroglian::YFP
DAPI
Mitotic stages
b
Phalloidin
Fas2
DAPI
Mitotic stages
c
Phalloidin
DAPI
Nrg-shRNA
d
Phalloidin
RFP
DAPI
Fas2G0336
e
Phalloidin
DAPI
Nrg-shRNA and UAS Inscuteable
f
Phalloidin
RFP
DAPI
Fas2G0336 and
UAS Inscuteable
g
0'
1'
CellMask
10'
40'
Fas2G0336 and UAS Inscuteable
h
Cells Above the Layer per Egg Chamber
140
120
100
80
60
40
20
0
*
**
ctrl
Inscuteable
ctrl
Inscuteable
Nrg RNAi
Fas2G0336
i

Supplementary Figure 1

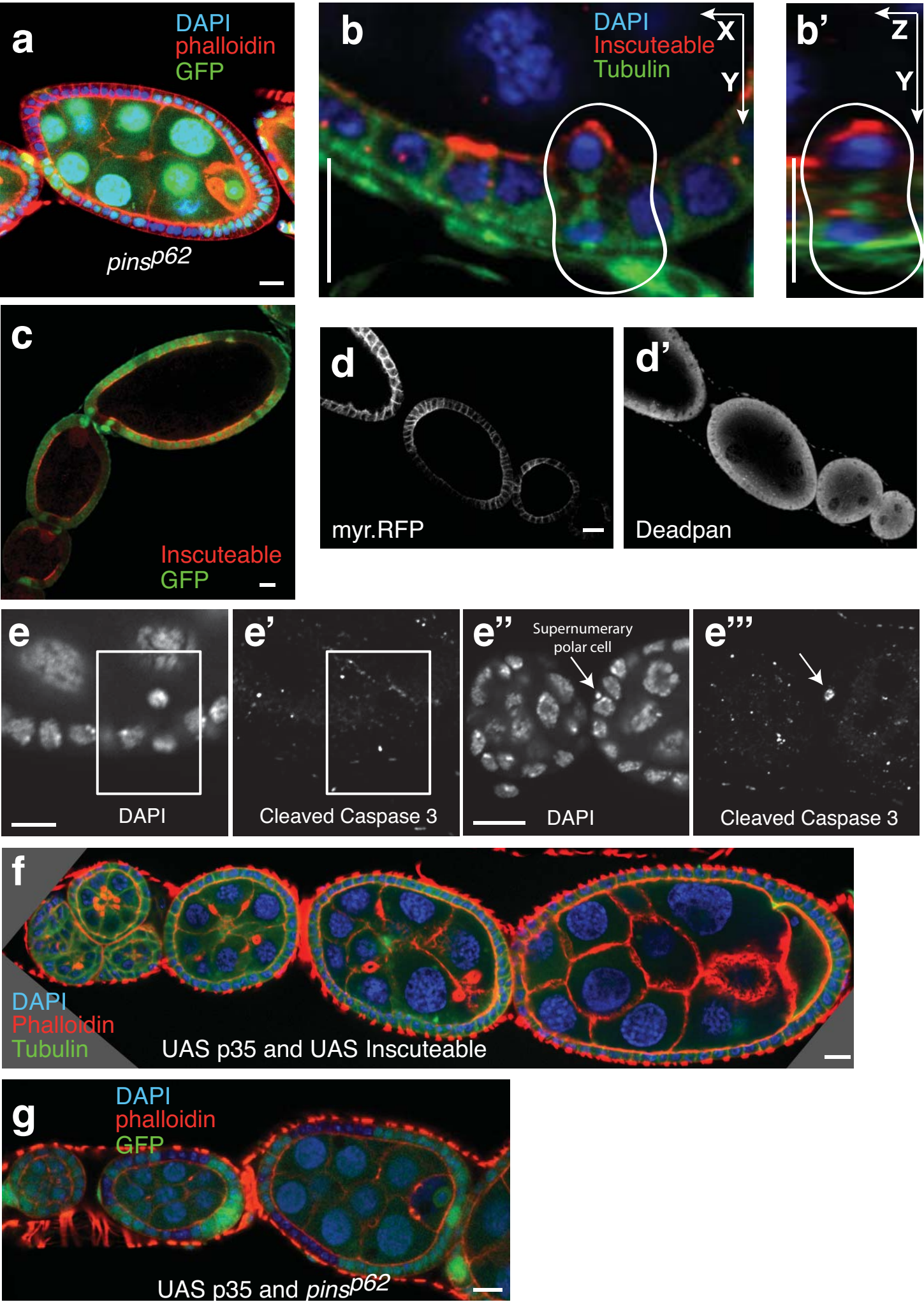

Supplementary Figure 2

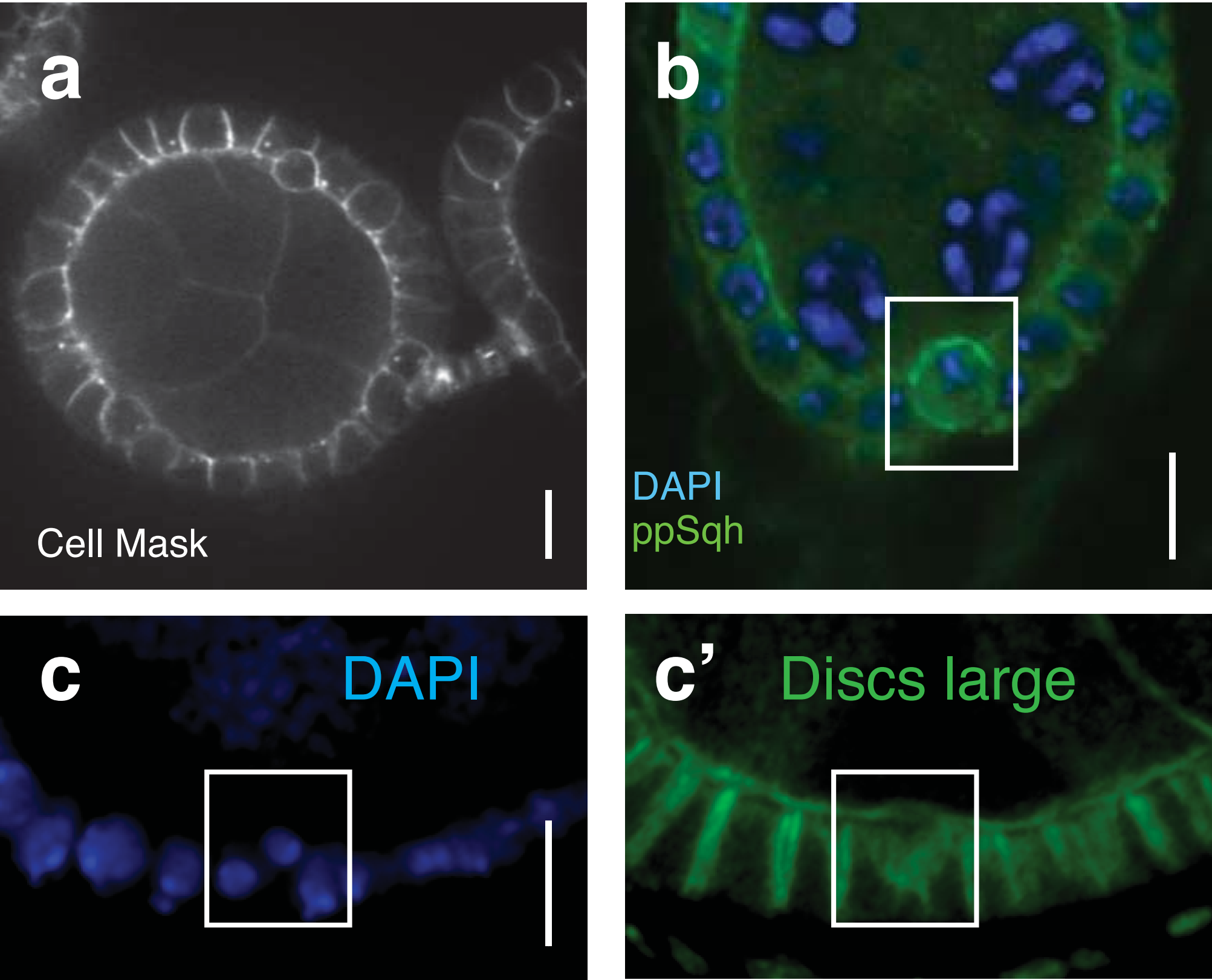

Supplementary Figure 3

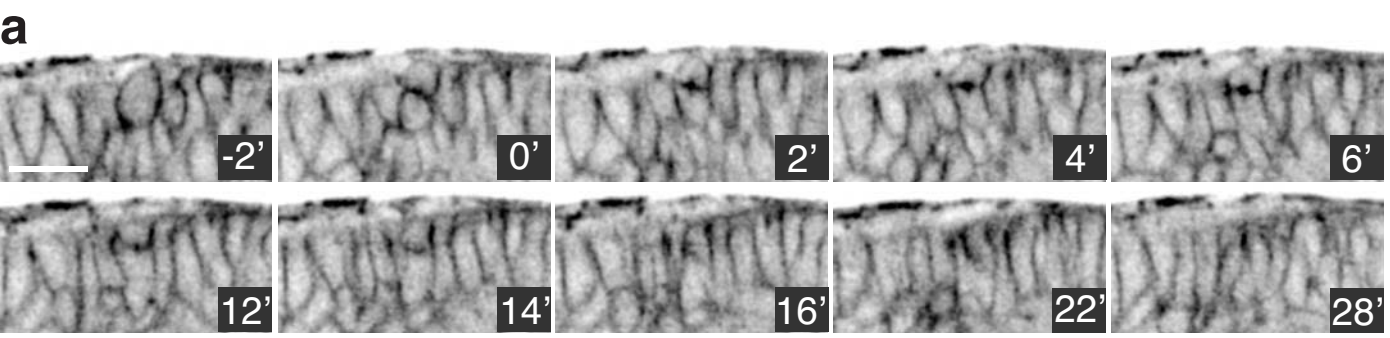

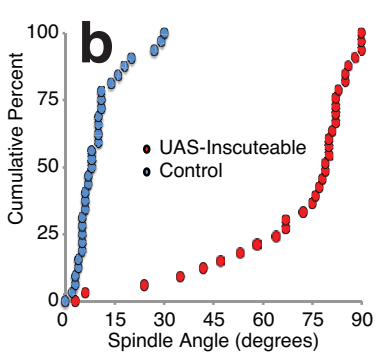

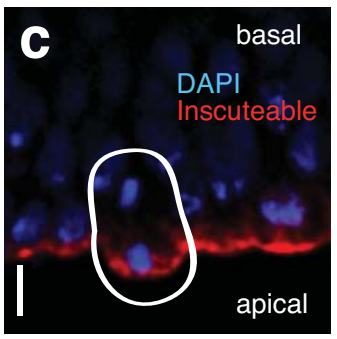

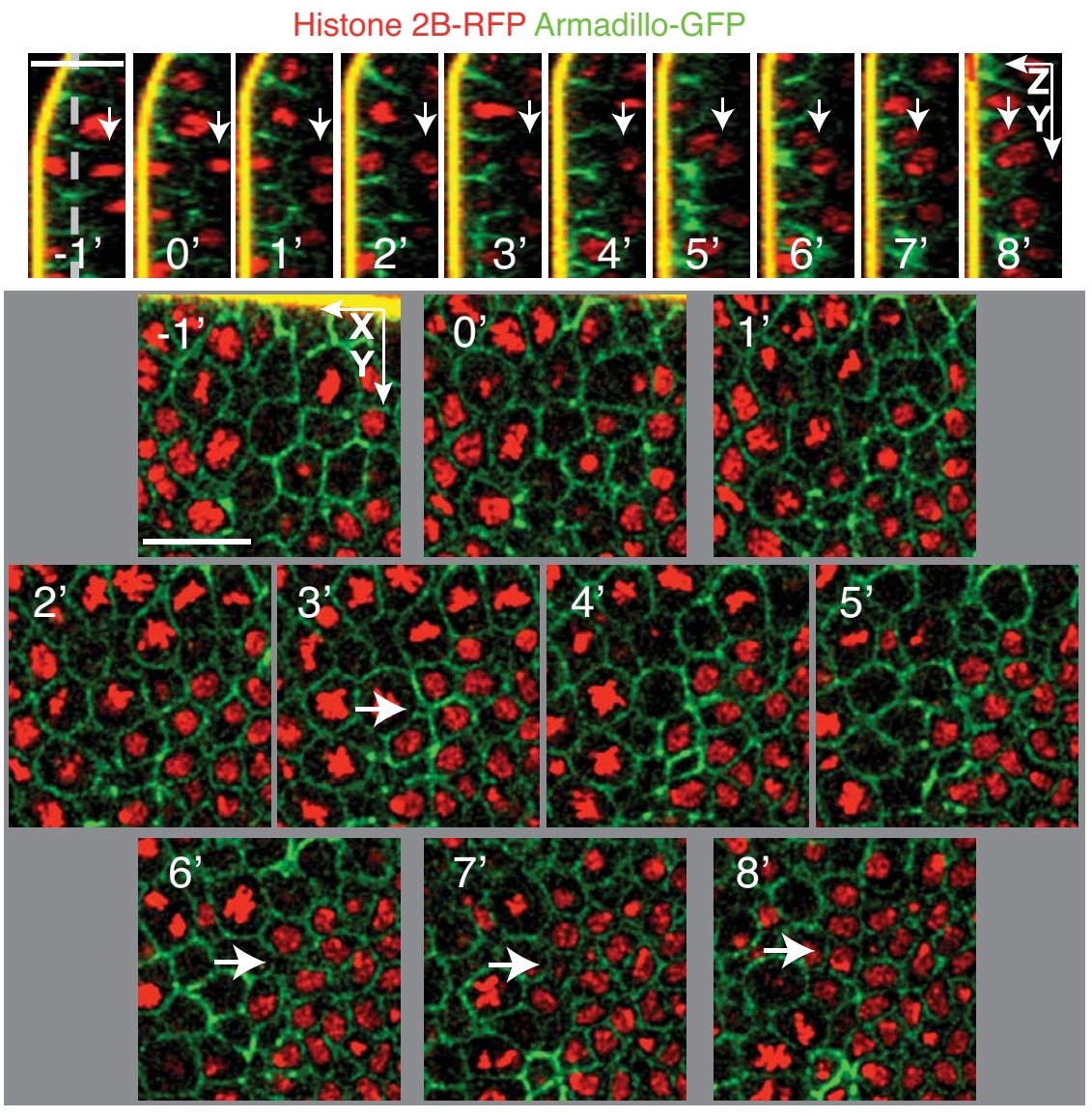

Supplementary Figure 4

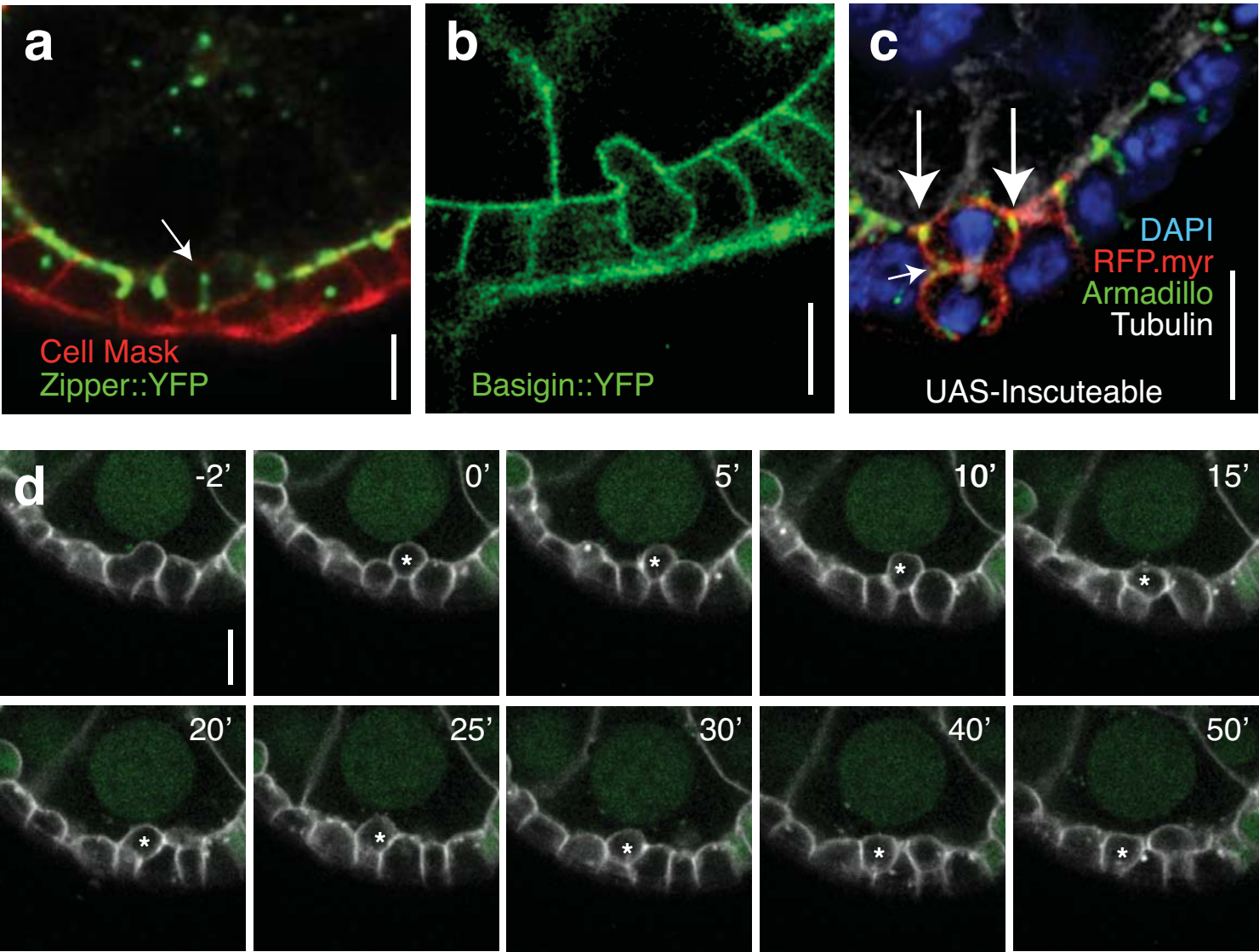

Supplementary Figure 5